

Bioinspired Growth of Crystalline Carbonate Apatite on Biodegradable Polymer Substrata

William L. Murphy[†] and David J. Mooney^{*}

Contribution from the Departments of Biomedical Engineering, Biologic and Materials Sciences, and Chemical Engineering, University of Michigan, Ann Arbor, Michigan 48109

Received October 25, 2001

Abstract: Mineralization in biological systems is a widespread, yet incompletely understood phenomenon involving complex interactions at the biomacromolecule–mineral nucleus interface. This study was aimed at understanding and controlling mineral formation in a poly(α -hydroxy ester) model system, to gain insight into biological mineralization processes and to develop biomaterials for orthopaedic tissue regeneration. We specifically hypothesized that providing a high surface density of anionic functional groups would enhance nucleation and growth of bonelike mineral following exposure to simulated body fluids (SBF). Polymer surface functionalization was achieved via hydrolysis of 85:15 poly(lactide-*co*-glycolide) (PLG) films. This treatment led to an increase in surface carboxylic acid and hydroxyl groups, resulting in a substantial increase in polymer surface energy from 42 to 49 dynes/cm². Treated polymers exhibited a 3-fold increase in heterogeneous mineral growth and growth of a continuous mineral film on the polymer surface. The mineral grown on PLG surfaces is a carbonate apatite, the major mineral component of vertebrate bone tissue. Mineral crystal size and morphology were dependent on the solution characteristics but unaffected by the degree of surface prehydrolysis. The mechanism of heterogeneous carbonate apatite growth was examined via ion binding assays, which indicated that calcium binding is mediated independently by the presence of soluble phosphate counterions and surface functional groups. These findings indicate that poly(α -hydroxy ester) materials can be readily mineralized using a biomimetic process, and that the impetus for mineral nucleation in this system appears more complicated than the simple electrostatic interactions proposed in previous biomineralization theory.

Introduction

Mineralization in biological systems is an elegant and structurally complex process involving ionic, stereochemical, and structural interactions at the biomacromolecule–mineral interface.^{1,2} A wide variety of organisms utilize diverse schemes to grow biominerals with functions ranging from magnetic sensing³ (magnetite in magnetotactic bacteria) to structural support⁴ (dahlite in vertebrate skeletons). The paradigm linking each biomineralization strategy is a supreme level of control over the physical chemistry of mineral growth. Mineralization during vertebrate bone growth is a classic example in which hydrophobic collagen fibrils are organized into parallel sheets with periodically staggered “hole zones”. These spaces are rich in phospho- and glycoproteins, creating a local charge accumulation.⁵ The anionic nature of the hole zone, along with

structural and stereochemical interactions, are thought to lead to attraction of calcium-rich mineral nuclei and initiation of mineral growth.^{6,7} A similar mechanism drives mollusk shell development, with hydrophobic β -chitin providing a substrate for deposition of acidic, anionic proteins that drive aragonite nucleation.^{6–9} In each case, an organic, hydrophobic material acts as a framework for deposition of an anionic, hydrophilic mineral nucleator that, in turn, drives mineral nucleation. Although the understanding of complex biological mineralization systems is incomplete and continues to grow, the fundamental mechanisms outlined above can be mimicked in synthetic systems to direct *ex vivo* biomineralization.

The highly controlled morphology, physical properties, and nanostructure of biological minerals have led to the development of biomimetic systems for controlled mineral formation *ex vivo*.^{10–16} The development of *ex vivo* systems is motivated

* Departments of Chemical Engineering, Biomedical Engineering, and Biologic and Materials Sciences, University of Michigan, 5213 Dental, 1011 North University Avenue, Ann Arbor, MI 48109-1078. Telephone: (734) 763-4816. Fax: (734) 763-0459. E-mail: mooneyd@umich.edu.

[†] Department of Biomedical Engineering, University of Michigan, 5210 Dental, 1011 North University Avenue, Ann Arbor, MI 48109-1078. Telephone: (734) 763-7215. Fax: (734) 763-0459. E-mail: wmurphy@engin.umich.edu.

(1) Mann, S.; Archibald, D. D.; Didymus, J. M.; et al. *Science* **1993**, *261*, 1286.
(2) Sarikaya, M. *Proc. Natl. Acad. Sci. U.S.A.* **1999**, *96*, 14183.
(3) Chasteen, N. D.; Harrison, P. M. *J. Struct. Biol.* **1999**, *126*, 182.
(4) Weiner, S.; Traub, W.; Wagner, H. D. *J. Struct. Biol.* **1999**, *126*, 241.
(5) Lee, S.; Veis, A. *J. Peptide Protein Res.* **1980**, *16*, 231.

(6) Lowenstam, H. A.; Weiner, S. *On Biomineralization*; Oxford University Press: New York, 1989.
(7) Weiner, S. *Crit. Rev. Biochem.* **1986**, *20*, 365.
(8) Weiner, S. *J. Chromatography* **1982**, *245*, 148.
(9) Sarikaya, M.; Liu, J.; Aksay, I. A. In *Biomimetics*; Sarikaya, M., Aksay, I. A., Eds.; AIP Press: Woodbury, NY, 1995; Chapter 3.
(10) Bunker, B. C.; Rieke, P. C.; Tarasevich, B. J.; et al. *Science* **1994**, *264*, 48–55.
(11) Xu, G.; Aksay, I. A.; Groves, J. T. *J. Am. Chem. Soc.* **2001**, *123*, 2196.
(12) Liu, G. J.; Miyaji, F.; Kokubo, T.; et al. *J. Mater. Sci. Mater. Med.* **1998**, *9*, 285.
(13) Dalas, E.; Kallitsis, J. K.; Koutsoukos, P. G. *Langmuir* **1991**, *7*, 1822.
(14) Murphy, W. L.; Kohn, D. H.; Mooney, D. J. *J. Biomed. Mater. Res.* **2000**, *50*, 50.

both by the desire to more completely understand biomineralization processes and by the potential utility of biominerals in industrial and biomedical applications. Prevalent strategies involve pragmatic presentation of polar functional groups that both increase local ion accumulation via electrostatic effects¹⁷ and decrease the energy at the organic substrate–mineral nucleus interface.¹⁸ In each case, the basic, biomimetic premise is that functional groups present in large quantities at the mineralization front in biological systems are capable of inducing mineral nucleation if presented in the appropriate fashion. Select model systems have been extended to biomedical applications, such as hydroxyapatite mineral growth on functionalized titanium¹⁹ and bioactive, ion-exchange glasses.²⁰ Carbonated hydroxyapatite is the major mineral component in human bone extracellular matrix,^{6,21} and bonelike mineral coatings appear to have pronounced effects on proper bone tissue development. More specifically, a bonelike mineral has been shown to be a prerequisite to bonding of orthopedic implant materials to native bone tissue²² (osteoconductivity), and may drive osteogenic differentiation of adult human stem cells^{23,24} (osteoinductivity). Despite the potential benefits of biominerals in regenerative medicine, few studies to date have been aimed at mineral formation on degradable biomaterials for use in orthopedic tissue regeneration.^{14,25}

The highly hydrophobic, yet hydrolytically degradable, poly-(α -hydroxy ester)²⁶ biomaterials may be suitable models for mineralization, as biological mineralization is thought to be induced by anionic functional groups within the framework of a hydrophobic template (i.e., collagen fibrils in vertebrate skeletons^{6,7} or β -chitin in invertebrate exoskeletons^{8,9}). Poly-(L-lactic acid) and various compositions of poly(lactide-co-glycolide) are particularly intriguing systems, as they have found widespread use in various biomedical applications,²⁶ including bone tissue regeneration.²⁷ In view of the functional analogies between some classes of biodegradable polymer and biological mineralization systems, this study is aimed at understanding and controlling the mineralization process on biodegradable polymer substrata.

Experiments and Methods

Film Preparation and Mineralization. PLLA and PLG pellets with lactide/glycolide ratios of 50:50, 75:25, and 85:15 (inherent viscosity = 0.8 ± 0.2) were obtained from either Alkermes, Inc., or Boehringer-Ingelheim, Inc. Films were prepared via a compression molding process in which pellets were placed between two smooth stainless steel plates heated above the T_m or T_g of each polymer composition (175 °C for 50:50, 190 °C for 75:25, 200 °C for 85:15, and 350 °C for PLLA).

Table 1. Advancing Contact Angles of Water and Diiodomethane on Various Poly(α -hydroxy Ester) Film Compositions^a

sample	advancing contact angle (°)		surface energy		
	water	diiodomethane	polar	dispersive	total
50:50 PLG	60.9 ± 4.1	42.4 ± 2.7	20.85	27.71	48.56
85:15 PLG	71.4 ± 1.7	47.9 ± 2.0	15.70	26.45	42.15
PLLA	79.6 ± 2.2	50.0 ± 1.5	11.55	26.72	38.27
85:15 ^b	62.0 ± 2.5	46.6 ± 2.7	20.94	26.02	46.96
85:15 ^c	59.7 ± 2.9	40.9 ± 2.7	21.34	28.20	49.54
85:15 ^d	60.5 ± 2.2	41.5 ± 1.4	20.92	28.05	48.97

^a Surface energy values were calculated using the contact angle measurements of each liquid. ^b Hydrolyzed for 10 min. ^c Hydrolyzed for 30 min. ^d Hydrolyzed for 60 min.

The plates were then pressed together at 1.0 MPa for 10 s, followed by release of pressure and rapid quenching to room temperature. This resulted in smooth, ~250- μ m thick polymer films.

Films were each incubated in a 50 mL solution of either simulated body fluid (SBF) for 16 days or modified simulated body fluid (mSBF) for 7 days for mineral growth. The solutions were replaced with freshly prepared solution daily to ensure adequate ionic concentrations for mineral nucleation and growth. SBF was prepared by dissolving the following reagents in deionized water: 141 mM NaCl, 4.0 mM KCl, 0.5 mM MgSO₄, 1.0 mM MgCl₂, 4.2 mM NaHCO₃, 2.5 mM CaCl₂, and 1.0 mM KH₂PO₄. The resulting SBF was buffered to pH = 7.4 with Tris-HCl, and was held at 37 °C for the duration of the incubation period. The mSBF solution is identical to SBF, except that the CaCl₂ and KH₂PO₄ concentrations are doubled, and the solution is held at pH = 6.8 to avoid homogeneous precipitation of CaP phases. Certain films were subjected to a hydrolysis treatment prior to SBF incubation. These samples were immersed in 0.5 M NaOH for various periods of time (5, 10, 30, and 60 min) to produce a hydrolyzed, carboxylic acid-rich surface.

Polymer Film Characterization. Polymer films were characterized by contact angle measurements (surface energy measurements) and calcium binding analysis prior to surface mineralization. Sessile drop measurements were made by advancing 10 μ L of one of two liquids (H₂O and diiodomethane) on the film and measuring the advancing contact angle using a goniometer. Four measurements were taken in different regions and averaged on each of five films per condition (Table 1). From these data, surface tensions were calculated using the harmonic mean approximation of Young's equation:²⁸

$$(1 + \cos \theta_i)(\gamma_i^d + \gamma_i^p) = 4 \left(\frac{\gamma_i^d \gamma_s^d}{\gamma_i^d + \gamma_s^d} + \frac{\gamma_i^p \gamma_s^p}{\gamma_i^p + \gamma_s^p} \right)$$

where θ_i is the advancing contact angle of liquid i on the polymer film surface, γ_i^p and γ_i^d are the polar and dispersive surface energy components of liquid i , and γ_s^p and γ_s^d are the polar and dispersive surface energy components of the polymer. For each film type, the values for γ_s^p and γ_s^d were solved for using pairs of liquid contact angle measurements from the two separate liquids and the known surface energies of water and diiodomethane.²⁸

Calcium ion binding to both 85:15 PLG films hydrolyzed for 60 min in 0.5 M NaOH and nonhydrolyzed films was measured at six separate calcium concentrations (0.01, 0.05, 0.1, 1, 5, and 10 mM). Eight circular polymer films ($r = 0.5$ cm) per condition were incubated in 24-well tissue culture plates in 2 mL solutions containing the aforementioned calcium concentrations in 150 mM NaCl buffered to pH = 7.4 with Tris held at 37 °C to maintain nearly physiological ionic strength, pH, and temperature during calcium binding studies. Additionally, both hydrolyzed and nonhydrolyzed films were incubated in solutions that also contained phosphate ions. The concentration of

- (15) D'Sousa, S. M.; Alexander, C.; Carr, S. W.; et al. *Nature* 1999, 398, 312.
- (16) Campbell, A. A.; Fryxell, G. E.; Linehan, J. C.; Graff, G. L. *J. Biomed. Mater. Res.* 1996, 32, 111.
- (17) Ngankam, P. A.; Lavallo, P.; Voegel, J. C.; et al. *J. Am. Chem. Soc.* 2000, 122, 8998.
- (18) Mann, S.; Ozin, G. A. *Nature* 1996, 382, 313.
- (19) Wen, H. B.; de Wijn, J. R.; Cui, F. Z.; de Groot, K. *J. Biomed. Mater. Res.* 1998, 41, 227.
- (20) Abe, Y.; Kokubo, T.; Yamamuro, T. *J. Mater. Sci.: Mater. Med.* 1990, 1, 233.
- (21) Posner, A. S. *Physiol. Rev.* 1969, 49, 760.
- (22) Hench, L. L. *J. Am. Ceram. Soc.* 1991, 74, 1487.
- (23) Ohgushi, H.; Caplan, A. I. *J. Biomed. Mater. Res. Appl. Biomat.* 1999, 48, 913.
- (24) Krebsbach, P. H.; Kuznetsov, S. A.; Satomura, K. *Transplantation* 1997, 63, 1059.
- (25) Zhang, R.; Ma, P. X. *J. Biomed. Mater. Res.* 1999, 45, 285.
- (26) Gilding, D. G. In *Biocompatibility of Clinical Implant Materials*; Williams, D. F., Ed.; CRC Press: Boca Raton, FL, 1981: Chapter 9.
- (27) Crane, G. M.; Ishaug, S. L.; Mikos, A. G. *Nat. Med.* 1995, 1, 1322.

(28) Wu, S. *Polymer Interface and Adhesion*; Marcel Dekker: New York, 1982.

phosphate was chosen so as to mimic the Ca/P ratio of physiologic solutions (2.5/1) for each of the six calcium concentrations. After a 48 h incubation, the amount of calcium bound to each film was calculated by subtracting the total calcium added to the solution from the amount of measured calcium remaining in solution. The concentration of calcium in each solution was determined using a previously described colorimetric calcium assay.²⁹

Analysis of Mineral Growth. The morphology, composition, and phase of biomineral grown on polymer substrata were analyzed qualitatively and quantitatively. A conductive gold coating was applied to the surface of each film via sputter coating, and samples were imaged under high vacuum using a Hitachi S-3200N SEM operating at 25 kV. An energy-dispersive X-ray detector (Noran SiLi detector) was used in conjunction with SEM for elemental analysis of mineral crystals.

Mineral growth was then quantitatively analyzed for all samples via a previously described colorimetric phosphate assay.^{29,30} In brief, following SBF incubation, films were dried and incubated in 5.0 M sulfuric acid solution for mineral dissolution (complete dissolution was verified qualitatively via light microscopy). A 1.0 mL aliquot of the dissolved solution was added to a 4.0 mL solution composed of 1.0 mL H₂O, 1.0 mL 10 mM ammonium molybdate, and 2.0 mL acetone. The amount of phosphate was quantitatively detected by measuring the absorbance of the 400 nm band on a UV-vis Spectrophotometer (Perkin-Elmer Lambda 12 UV/VIS). Standards for the quantitative determination of phosphate content had a correlation coefficient greater than or equal to 0.999 for the concentration range 60–300 μ M.

To gain insight into the phase of the mineral grown, mineralized films were lyophilized and analyzed without further preparation in a Rigaku rotating anode system using Cu K α radiation. X-ray diffraction spectra were taken for 2θ angles from 20° to 50° at a scan rate of 2°/min.

Fourier transform IR spectroscopy (FTIR) data were obtained using an Avatar 360 FTIR ESP spectrometer (Nicolet Instrument Corp.). After mineralization in SBF, polymer films were mechanically ground, and 20 mg of the resulting particulate suspension was pressed into a KBr pellet and analyzed. The mineral formed via the mSBF process, because it was of appreciable thickness, was scraped from the surface of the polymer film, pressed into a KBr pellet, and analyzed. Spectra were obtained for 60 min prehydrolyzed PLG films incubated either in SBF for 16 days or mSBF for 7 days.

In all assays, 4–10 films were prepared, treated, and analyzed per condition, and statistical analysis was performed using InStat software, version 2.01. Values on graphs represent means and standard deviations.

Results

Surface Energies of Biodegradable Polymer Substrata. Surface hydrolysis and compositional variation of poly(α -hydroxy ester) films result in substantial changes in polymer film surface energy. Advancing contact angles of water and diiodomethane (DIM) display significant decreases (increased surface energy) after a 10 min hydrolysis treatment (Table 1). Contact angles continue to decrease with enhanced hydrolysis treatment time, culminating with decreases of 10.9° with H₂O and 6.4° with DIM. Surface energies calculated using the harmonic mean approximation of Young's equation showed an increase of 6.82 dynes/cm² after a 60 min hydrolysis treatment due largely to variation in the polar surface energy component (Table 1). Increases in PLG surface energy with alkaline treatment time can be attributed to an increase in the number of carboxylic acid endgroups formed upon hydrolytic surface functionalization. Increases in the lactide/glycolide ratio of the films lead to an increase in advancing contact angle (decreased surface

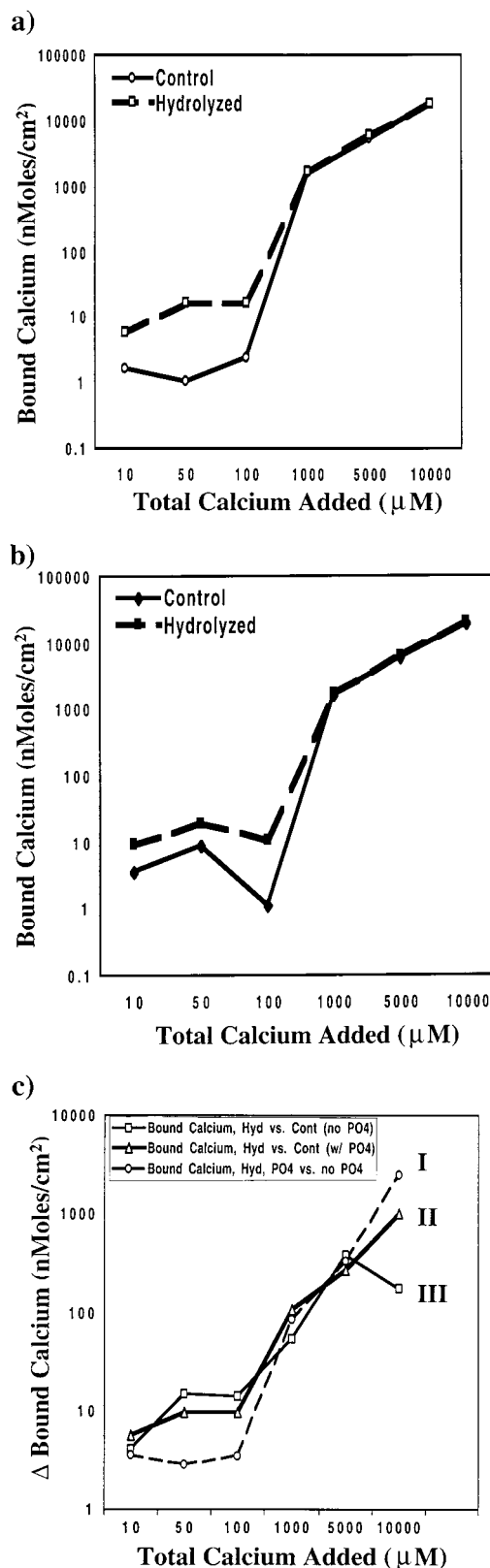


Figure 1. Binding of calcium ions to 85:15 PLG films measured in (a) absence and (b) presence of soluble phosphate ions for hydrolyzed and nonhydrolyzed films. (c) Data points indicating the difference between calcium bound to hydrolyzed substrates and nonhydrolyzed substrates in the presence (curve II) and absence (curve III) of phosphate ions. Curve I in part c indicates the difference between calcium bound to hydrolyzed films in the presence of phosphate ions and in the absence of phosphate ions.

(29) Murphy, W. L.; Messersmith, P. B. *Polyhedron* 2000, 19, 357.

(30) Heinonen, J. K.; Lahti, R. *J. Anal. Biochem.* 1991, 113, 313.

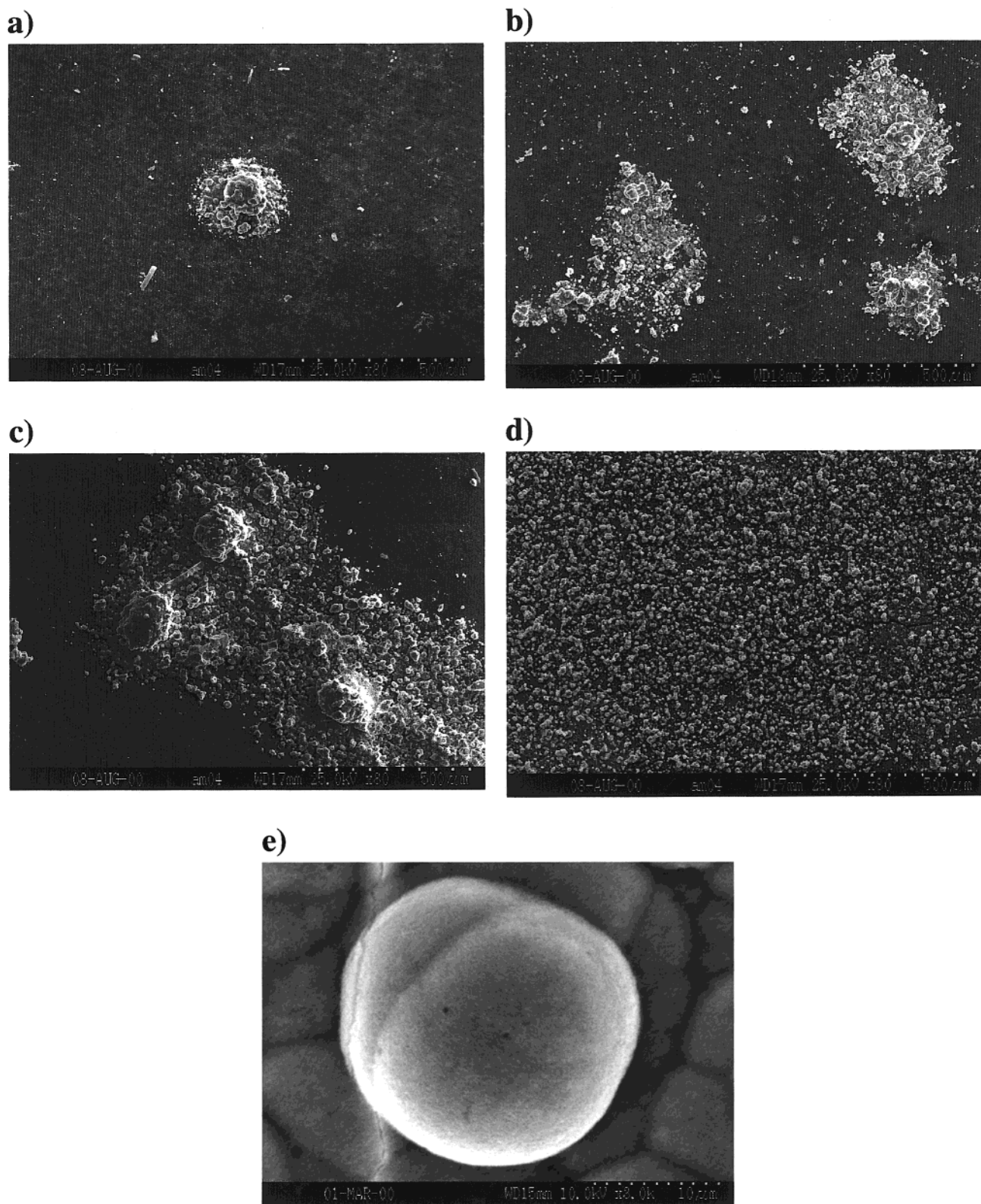


Figure 2. Electron micrographs of mineral formed on 85:15 PLG films via a 16 day incubation in SBF. Films pretreated in 0.5 M NaOH for (a) 0, (b) 5, (c) 30, and (d) 60 min (original magnification $\times 80$). (e) Mineral displayed a spherulitic microstructure in all conditions (original magnification $\times 3000$).

energy) of both H_2O and DIM. Again, the change in surface energy is largely reflected in the polar surface energy component (Table 1). The decrease in surface energy with enhanced lactide/glycolide ratio can be attributed to an increase in the density of surface methyl groups associated with the lactide component,

as the inherent viscosities of each polymer composition were nearly identical (0.8 ± 0.2 dL/g).

Ion Binding Analyses. Binding assays were undertaken to determine the effects of surface chemistry and solution characteristics on surface accumulation of calcium ions and gain

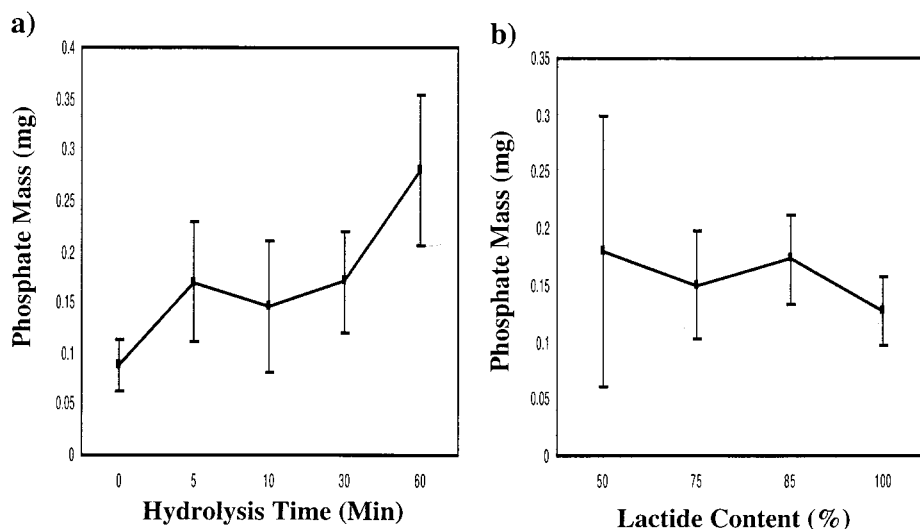


Figure 3. Phosphate content as a quantitative measure of mineral grown on (a) 85:15 PLG films after varying prehydrolysis treatment time or (b) poly(α -hydroxy ester) films with varying lactide/glycolide ratio. Mineral films were grown via a 16 day incubation in SBF.

insight into the mechanism for heterogeneous mineral nucleation. Variation in surface chemistry via hydrolytic surface functionalization had a pronounced effect on calcium binding to PLG films, both in the presence and absence of soluble phosphate ions. The amount of calcium binding to nonhydrolyzed films was significantly less than calcium binding to hydrolyzed films for each calcium concentration, with or without phosphate ions present (Figure 1a,b). In addition, the difference in calcium bound to hydrolyzed films vs nonhydrolyzed films increases with increasing calcium concentration (Figure 1c). This difference does not depend on the presence of phosphate ions, as curves II and III do not vary significantly (Figure 1c). The amount of calcium binding to hydrolyzed films with no phosphate was significantly less than calcium binding to hydrolyzed films with phosphate for each calcium concentration (Figure 1c, curve I). The effect of phosphate presence on calcium binding is less substantial than the effect of surface hydrolysis at lower calcium concentrations, but has a greater effect on calcium binding at high calcium concentrations. Interestingly, the differences in calcium binding induced by surface hydrolysis (curves II and III) and phosphate presence (curve I) are on the same order of magnitude and display the same general trends with variation in free [Ca].

Analysis of Heterogeneous Biomineral Growth. Next, heterogeneous mineralization on various poly(α -hydroxy ester) films was analyzed to determine the effects of surface chemistry and solution characteristics on the extent of mineral growth. Pretreatment of PLG films in 0.5 M NaOH led to clear differences in the ability of film surfaces to support heterogeneous mineral nucleation and growth. Films incubated in SBF for 16 days without prehydrolysis treatment displayed growth of isolated biomineral islands approximately 250 μ m in diameter (Figure 2a). Films that were prehydrolyzed for 5 and 30 min prior to a 16 day SBF incubation displayed increasing biomineral surface coverage (Figure 2b,c). Films pretreated for 60 min display growth of an essentially continuous mineral layer (Figure 2d). The microcrystalline morphology of the biomineral crystals is spherulitic and remains the same regardless of prehydrolysis treatment (Figure 2e).

The qualitative increases in mineral surface coverage with prehydrolysis time displayed in electron micrographs were then

quantitated. Prehydrolyzed, mineralized films demonstrated a significant increase in phosphate content with prehydrolysis time, culminating in a 3-fold increase with a 60 min prehydrolysis treatment (Figure 3a). The mass of phosphate on 5 min prehydrolyzed films was significantly greater than phosphate mass on films that were not pretreated. Analysis of variance of phosphate mass changes on prehydrolyzed, mineralized films reveals a significant difference in phosphate mass with increased prehydrolysis time ($p < 0.05$). In contrast, PLG films with differential lactide/glycolide ratio showed no significant variation in surface mineralization (Figure 3b). These data, along with the polymer surface chemistry results, indicate that the driving force for mineralization is not simply an increased polymer surface energy. Rather, they assert that the carboxylic acid and hydroxyl groups available upon hydrolytic surface functionalization are specifically involved in mineral nucleation, partly through interaction with soluble calcium ions or calcium-containing mineral prenuclei.

Mineral growth experiments were then performed within a modified simulated body fluid (mSBF) to determine whether increasing the potential for calcium ion binding to PLG surfaces (high ion concentrations) would lead to enhanced heterogeneous mineral growth. Films incubated in mSBF without prehydrolysis treatment did not display growth of biomineral (Figure 4a), whereas 60 min prehydrolyzed films showed growth of a continuous biomineral film (Figure 4b). The mineral grown in the mSBF process displays a thin, platelike crystalline morphology (Figure 4c).

Analysis of Mineral Phase and Composition. To confirm the growth of a bonelike mineral film and examine differences in the phase and composition of mineral formed in the SBF and mSBF processes, X-ray diffraction (XRD) and Fourier transform infrared (FTIR) spectroscopy were next performed. These analyses indicate that the mineral formed on 85:15 PLG films is carbonated and apatitic, and they confirm that crystal size is dependent on the characteristics of the mineral growth solution. Mineralization treatment using SBF results in the appearance of two well-defined XRD peaks associated with carbonate hydroxyapatite (Figure 5). The mineral grown via incubation in mSBF was also apatitic, displaying similar XRD peaks. However, the mineral grown in the mSBF process contains a

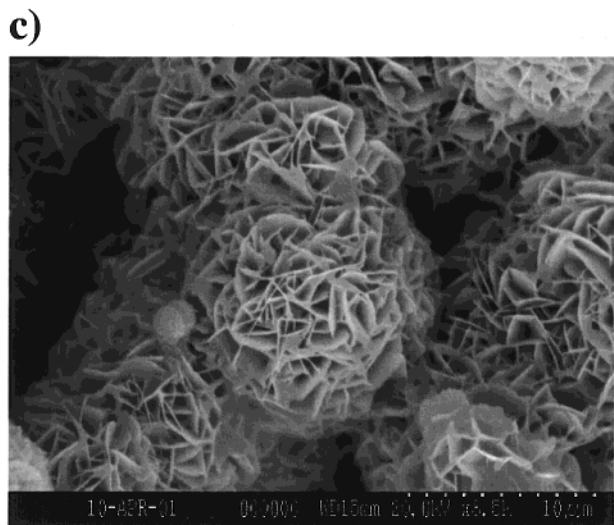
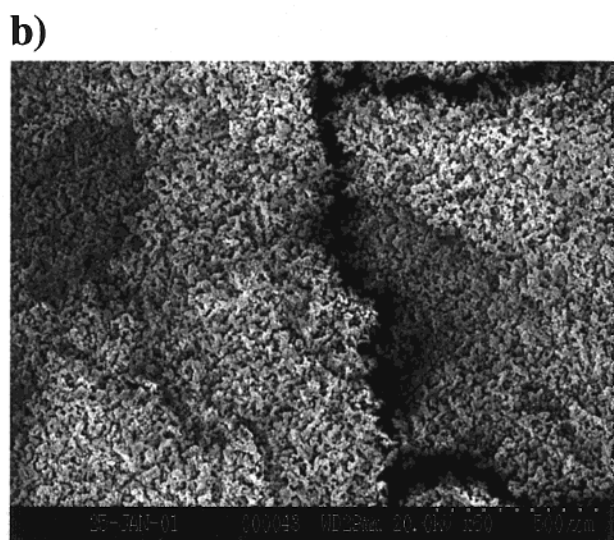
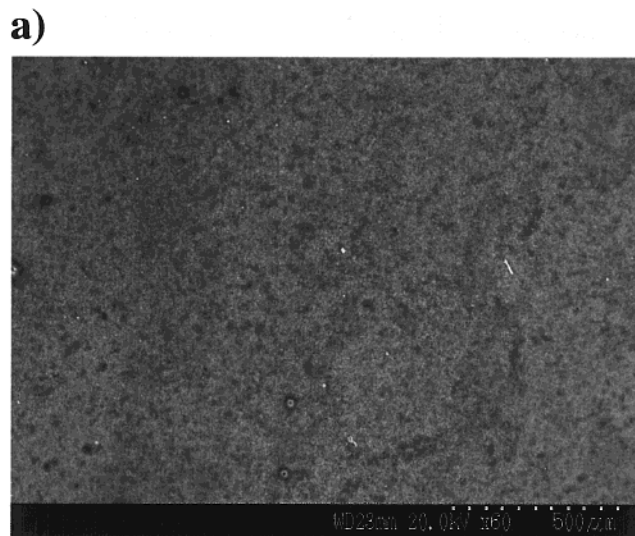


Figure 4. Electron micrographs of the surface of 85:15 PLG films incubated for 7 days in mSBF after (a) no prehydrolysis or (b) a 60 min prehydrolysis (original magnification $\times 60$). (c) Mineral displayed a platelike nanostructure (original magnification $\times 3500$).

peak at 26° associated with the 002 reflection from carbonate hydroxyapatite, whereas the 002 peak in the spectrum of the

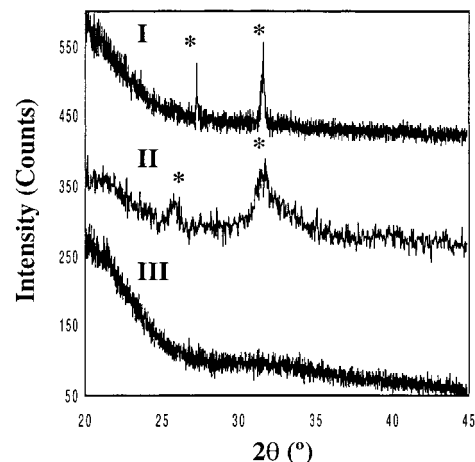


Figure 5. X-ray diffraction spectra of 60 min prehydrolyzed 85:15 PLG films: (I) mineralized via a 16 day incubation in SBF, (II) mineralized via a 7 day incubation in mSBF, or (III) nonmineralized. Peaks associated with hydroxyapatite mineral growth are denoted by *.

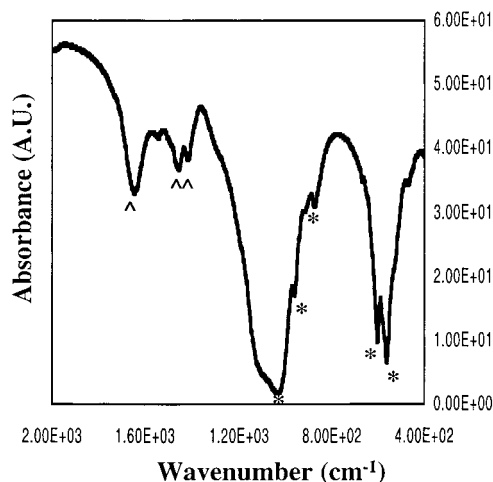


Figure 6. Fourier transform infrared spectra of mineral scraped from 85:15 PLG films. Films were prehydrolyzed for 60 min, and incubated in mSBF for 7 days, to achieve mineral growth. Peaks associated with apatitic phosphate are denoted by *, and peaks associated with carbonate substitution in the apatite crystals are denoted by ^.

mineral grown in the SBF process appears at 27° . Similar small differences in the d spacings of 002 planes have been noted in natural and synthetic carbonate apatites.³¹ In addition, the broadened peak areas in the mSBF sample spectrum are indicative of the small crystal size of the platelike biomineral (Figure 4c) relative to the spherulitic biomineral grown via incubation in SBF (Figure 2e). Importantly, prehydrolysis treatment has no apparent effect on the phase of the biomineral grown on PLG, as XRD spectra of mineral grown after each prehydrolysis time displayed identical peaks (not shown). The FTIR spectrum of mineral grown using the mSBF process displays absorbance peaks associated with apatitic phosphate groups, and peaks associated with carbonate substitution (Figure 6). Similar peaks were present in the SBF mineral spectrum (not shown). The FTIR spectrum of each mineral is indicative of a carbonated apatite mineral similar to the major mineral component of vertebrate bone tissue.

(31) *Powder Diffraction File: Inorganic Phases*, JCPDS International Centre for Diffraction Data: Swarthmore, PA, 1987.

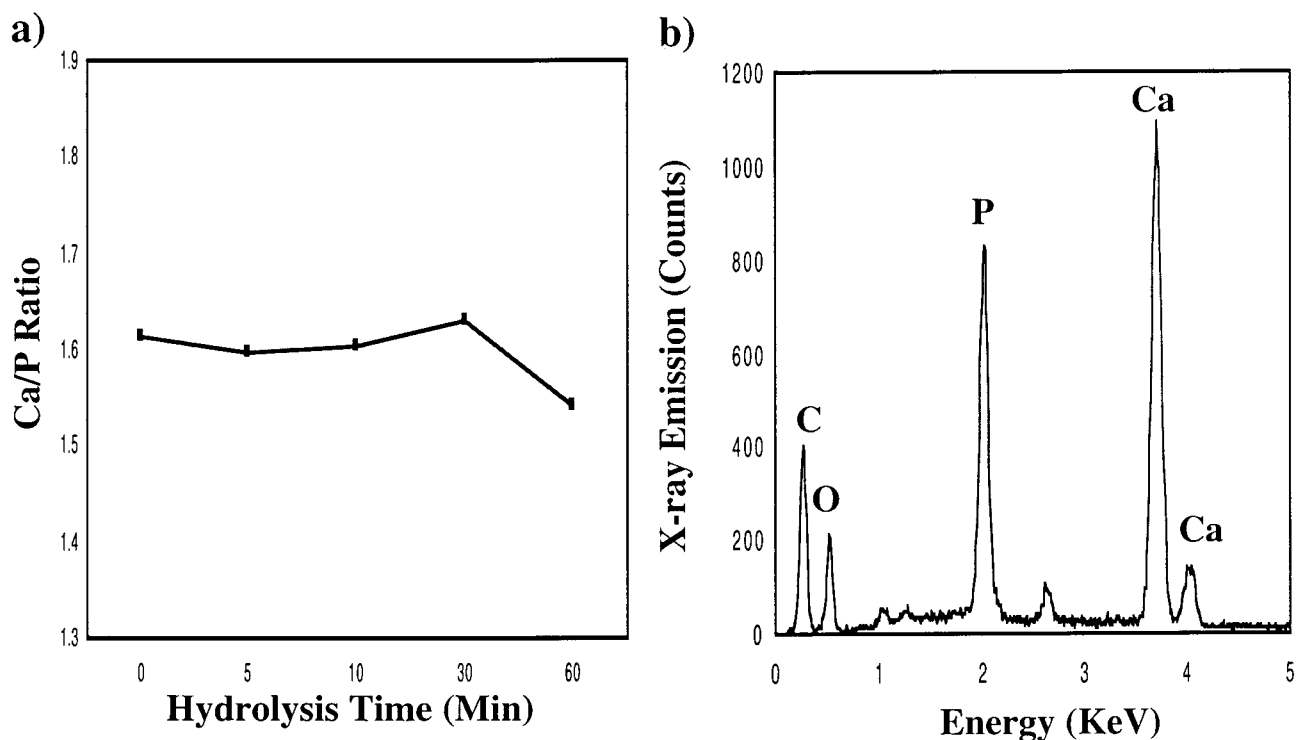


Figure 7. (a) Calcium/phosphorus ratios of mineral grown on 85:15 PLG films after various prehydrolysis treatment times. (b) Typical EDS spectrum of biomineral grown via incubation in SBF.

Compositional analyses were performed on mineral formed via both the SBF and mSBF processes to determine the effects of surface prehydrolysis on the composition of the mineral formed and to further confirm the growth of a bonelike apatite mineral. Energy-dispersive X-ray spectroscopy (EDS) of the SBF mineral after various prehydrolysis times indicates that prehydrolysis treatment has no appreciable effect on the elemental composition of the mineral (Figure 7). The calcium/phosphorus ratio remains 1.6 ± 0.04 for all prehydrolysis conditions, suggesting that the mineral grown is a bonelike apatite mineral in all cases. The mineral grown via the mSBF process had a Ca/P of 1.55, also suggesting the growth of a bonelike apatite.

Discussion

Surface hydrolysis of poly(α -hydroxy ester) films results in enhanced polymer surface energy, indicative of an increase in the amount of surface carboxylic acid and hydroxyl groups (Table 1). Hydroxide ions in alkaline solution react with ester bonds in the backbone of the polymer films resulting in chain scission and leaving hydrophilic carboxylic acid and hydroxyl groups on the polymer film surface. Poly(α -hydroxy ester) surface energy could also be enhanced by decreasing the lactide/glycolide ratio, thereby increasing the concentration of surface methyl groups. The measured surface energy of PLLA is identical to that of previous studies,³² and the effects of alkaline hydrolysis on surface functionalization is consistent with other studies using poly(glycolic acid) meshes for vascular tissue engineering.³³

The concentration of carboxylic acid and hydroxyl groups, enhanced via alkaline hydrolysis, regulates calcium binding and

heterogeneous biomineral growth on PLG films. Calcium binding curves indicate that both the total amount of calcium bound (Figure 1a,b) and the difference between calcium bound to hydrolyzed versus control films (Figure 1c) are more pronounced with increasing total solution calcium concentration, and that all surface-associated, calcium-binding groups are not saturated at the highest calcium concentration used ($[Ca] = 10$ mM). In turn, the extent of heterogeneous biomineral growth at the ionic concentrations of human blood plasma is enhanced with surface hydrolysis (Figures 2, 3a), likely due to interactions between polar functional groups on the surface and ionic precursors in solution. Both carboxylic acid groups^{5,8,16,34} and hydroxyl groups^{12,20} have been implicated in directing nucleation of apatite minerals in previous studies. The dependence of mineral growth on surface hydrolysis could potentially be explained by implicating the effects of decreased polymer surface energy on ordered water structure at the macromolecule-mineral nucleus interface, as in previous studies of $CaCO_3$ nucleation using surfactants such as poly(vinyl alcohol).³⁵ However, there is no significant difference in the amount of mineral formed on poly(α -hydroxy ester) films of variable composition (Figure 3b), which show similar differences in surface energy to hydrolyzed 85:15 PLG surfaces (Table 1). Therefore, it is more likely that nucleation of biomineral on the surface of hydrolyzed PLG films is directed by calcium binding in the presence of phosphate ions, as suggested by the calcium binding data (Figure 1).

The presence of phosphate ions in solution also regulates calcium ion binding to PLG surfaces. At all calcium concentrations, there was a significant increase in calcium binding to

(32) Irvine, D. J.; Ruzette, A. G.; Mayes, A. M.; Griffith, L. G. *Biomacromolecules* 2001, 2, 545.

(33) Gao, J.; Niklason, L.; Langer, R. J. *Biomed. Mater. Res.* 1998, 42, 417.

(34) Naka, K.; Chujo, Y. *Chem. Mater.* 2001, 13, 3245.

(35) Didymus, J. M.; Oliver, P.; Mann, S.; et al. *J. Chem. Soc., Faraday Trans.* 1993, 89, 2891.

hydrolyzed PLG films in the presence of soluble phosphate ions, and the difference in calcium binding caused by phosphate ion presence is more pronounced at higher ion concentrations (Figure 1c). It is interesting to note that the increases in binding caused by phosphate ion presence is on the same order of magnitude as the increases caused by surface hydrolysis. This is particularly clear at soluble calcium concentrations in the physiological range (1 and 5 mM). Thus, the mechanisms involved in regulation of calcium ion binding by surface functional groups and phosphate ion presence may be similar, although they appear to occur independently, as described below.

The positive effect of surface hydrolysis on calcium binding is similar in the presence or absence of phosphate ions (Figure 1c). This phenomenon is most apparent at 1 and 5 mM calcium concentrations, which approximate physiologic calcium concentrations ($[\text{Ca}]_{\text{plasma}} = 2.5 \text{ mM}$). This is somewhat surprising in light of current biomineralization theory, which implicates electrostatic interactions between calcium ions, soluble phosphate ions, and immobilized functional groups as a key initial step in heterogeneous mineral growth^{1,6–7,9,18}. One would expect that the effects of phosphate ion presence and surface functionality would be linked in the poly(α -hydroxy ester) system if initial calcium ion chelation was driven exclusively by ionic interactions (i.e., the effect of surface hydrolysis on calcium binding would differ in the presence of phosphate counterions). Rather, calcium ion sequestration in the near surface region is likely regulated and stabilized by more complex interactions between calcium and phosphate ion-rich nuclei and surface functional groups on the PLG surface. This may have implications for in vivo biomineralization systems such as vertebrate tooth and bone mineralization in which immobilized, negatively charged functional groups, calcium ions, and phosphate ions also interact in the initial stages of mineral nucleation.

The minerals grown in both the SBF and mSBF processes are carbonate apatites, with crystal size and morphology dependent on the ionic concentrations in the mineral growth solution. Ca/P ratios (Figure 7) and peaks in the X-ray diffraction (Figure 5) and FTIR (Figure 6) spectra are consistent with previous studies on biological apatites,³⁶ specifically bone mineral.²¹ In each case, crystals appear to be oriented randomly without preferred orientation (Figures 2, 4). This is not surprising, as there was no attempt in this study to controllably inhibit growth of the crystals in particular directions via the use of charged additives, as in previous controlled crystallization studies.³⁴ The carbonate apatite mineral with very thin, platelike crystals grown via the mSBF process is particularly similar to bone apatite in its crystal structure (Figure 5), Ca/P ratio (1.55), and morphology (Figure 4), which suggests that the mSBF process may be ideally suited for growth of mineral substrata for biomedical applications.

Although other approaches have been described to functionalize surfaces for ex vivo biomineralization,^{10–16,37–40} simple

hydrolytic functionalization represents a relatively simple, efficient, and controllable method that may find widespread applicability in biomaterials development for bone regeneration. The concept of hydrolytic functionalization is immediately applicable to several other existing biomaterial systems, such as poly(anhydrides), poly(carbonates), and other poly(esters), which leave carboxylic acid endgroups upon hydrolytic degradation. Furthermore, the extent of surface functionalization in the poly(α -hydroxy ester) system does not affect the composition (Figure 7) or morphology (Figure 2a–d) of the mineral grown, which suggests that platelike or spherulitic carbonate apatites could be grown in other systems using the methods described herein. Like the poly(α -hydroxy ester) system, these other biomaterials may be well suited for use in orthopedic regenerative medicine, in which combinations of degradable materials, cells, and inductive biological molecules are tailored to direct development of human bone tissue.⁴¹ Several processing methods exist to fabricate porous, three-dimensional structures using poly(α -hydroxy esters), perhaps making this system particularly applicable to 3-D bone tissue regeneration.¹⁴

Conclusions

As in complex biological systems, the process of mineral growth on biodegradable polymers can be augmented and controlled by variation in the functional groups present at the mineral nucleation site or the ionic characteristics of the mineral growth environment. Surface hydrolysis of poly(α -hydroxy esters) results in an increase in the amount of surface carboxylic acid and hydroxyl groups due to scission of polyester chains. The presence of these groups regulates calcium binding to the polymer surface and heterogeneous mineral growth. The presence of phosphate ions in solution also regulates calcium binding to PLG surfaces, and although the effect of phosphate ion presence on calcium binding is on the same order of magnitude as the effect of surface functionality, the two effects appear to be independent. The composition of the mineral grown in both the SBF and mSBF solutions is a carbonate apatite similar to vertebrate bone mineral, with crystal size and morphology dependent on solution characteristics, but not dependent on polymer surface characteristics.

Acknowledgment. The authors acknowledge technical assistance from Katherine A. Gilhool and Julie Spence. The authors are grateful for financial support from the NIH (R01 DE13033). They also acknowledge the NIH for a cellular biotechnology training grant (T32 GM 08353) to W.L.M.

JA012433N

- (37) Tanahashi, M.; Matsuda, T. *J. Biomed. Mater. Res.* **1997**, *34*, 305.
- (38) Mann, S.; Heywood, B. R.; Rajam, S.; et al. *J. Phys. D: Appl. Phys.* **1991**, *3*, 154.
- (39) Heywood, B. R.; Mann, S. *Chem. Mater.* **1994**, *6*, 311.
- (40) Tretinnikov, O. N.; Kato, K.; Ikada, Y. *J. Biomed. Mater. Res.* **1994**, *28*, 1365.
- (41) Yaszemski, M. J.; Payne, R. G.; Hayes, W. C.; et al. *Biomaterials* **1996**, *17*, 175.

(36) Elliot, J. C. *Structure and Chemistry of the Apatites and the Other Calcium Orthophosphates*; Elsevier Science: Amsterdam, 1994.